




# Homoharringtonine Exerts an Antimyeloma Effect by Promoting Excess Parkin-Dependent Mitophagy


This article was published in the following Dove Press journal:  
*Drug Design, Development and Therapy*

Yanyu Zhang <sup>1</sup>

Ning Huang <sup>2</sup>

Jie Xu<sup>3</sup>

Wei Zheng <sup>3</sup>

Xing Cui <sup>3</sup>

<sup>1</sup>Department of Traditional Chinese Medicine, Shandong University of Traditional Chinese Medicine, Jinan, People's Republic of China; <sup>2</sup>Clinical Laboratory Department, Affiliated Hospital of Shandong University of Traditional Chinese Medicine, Jinan, People's Republic of China; <sup>3</sup>Department of Hematology, Affiliated Hospital of Shandong University of Traditional Chinese Medicine, Jinan, People's Republic of China

**Purpose:** Homoharringtonine (HHT) has been used as an antileukemia agent in the clinic which processes a high-potential therapeutic efficacy against multiple myeloma (MM). In this study, we investigated the antimyeloma mechanism of HHT.

**Methods:** Three MM cell lines and a xenograft model were applied. Mitochondrial function was evaluated by detecting MitoTracker Green, the mtDNA copy number, mitochondrial protein and enzyme activity, the mitochondrial membrane potential and mitochondrial morphology. Mitophagy levels were assessed by monitoring autophagosomes, performing a colocalization analysis and determining the levels of related proteins. An shRNA was applied to knockdown *Parkin*.

**Results:** Based on the results of the in vitro experiments, HHT exerted a promising anti-proliferative effect on the MM.1S, RPMI 8226 and H929 cell lines by increasing mitophagy. In addition, HHT markedly inhibited myeloma tumor growth and prolonged survival by promoting mitophagy in vivo. Furthermore, HHT treatment contributed to notable mitochondrial dysfunction and Parkin-dependent mitophagy, as evidenced by the destruction of mitochondria, the decrease in the mtDNA copy number, decrease in the Bcl-2/Bax ratio, and decrease in the levels of mitochondrial proteins and the optimal expression of Parkin and NDP52. However, the addition of rapamycin did not produce significant synergistic effect with HHT, indicating that HHT reached the threshold level to induce mitophagy. The colocalization analysis and assessment of mitochondrial function examination further confirmed that HHT triggered mitophagy and mitochondrial dysfunction. Moreover, the anti-proliferative effect of HHT was reversed by an shRNA targeting *Parkin*, highlighting the indispensable role of Parkin-dependent mitophagy in the antimyeloma effect of HHT.

**Conclusion:** HHT exerts an antimyeloma effect by inducing excess mitophagy, providing new mechanistic insights into a therapeutic strategy for MM.

**Keywords:** homoharringtonine, multiple myeloma, mitophagy, *Parkin*, mitochondrial dysfunction

## Introduction

Multiple myeloma (MM) is the second most prevalent hematological malignancy among adults and is characterized by the clonal proliferation of plasma cells.<sup>1</sup> The emergence of new therapeutic agents, such as proteasome inhibitors and immunomodulatory agents, has improved survival rates among patients with MM. However, MM is a refractory disease, and these therapies still have several limitations and challenges, including high relapse rates, the development of resistance and toxicity.<sup>2</sup> Therefore, novel treatment strategies are urgently needed.

Autophagy is a crucial mechanism for intracellular homeostasis, as it degrades proteins, lipids, polysaccharides and other intracellular components

Correspondence: Xing Cui  
Department of Hematology, Affiliated Hospital of Shandong University of Traditional Chinese Medicine, Jinan, Shandong Province 250014, People's Republic of China  
Tel/Fax +86 68616042  
Email cdz45@foxmail.com

and regulates energy metabolism.<sup>3</sup> Mitophagy is a type of selective autophagy that plays an important role in the quality control of the mitochondrial network through the engulfment of dysfunctional and redundant mitochondria.<sup>4</sup> Since mitochondrial and metabolic alterations are critical in cancer progression,<sup>5</sup> the regulation of mitochondrial functions is crucial during treatment. In addition, mitochondria converge on several overlapping pathways consisting of the regulation of mitophagy, tumorigenesis, and cell death.<sup>6</sup> Hence, the regulation of mitophagy and mitochondrial function is expected to serve as a therapeutic target in cancer, including MM. However, mitophagy exerts complex effects on cancer;<sup>7</sup> on the one hand, mitophagy exerts prosurvival effects on tumors by eliminating defunct mitochondria and maintaining metabolism. On the other hand, excess mitophagy might lead to mitophagic cell death due to the loss of normal mitochondria and the lack of energy metabolism.<sup>8</sup> Moreover, mitophagy has been reported to induce cell death through interactions with other mechanisms, such as apoptosis and necroptosis.<sup>9,10</sup> Thus, the specific role of mitophagy varies in different tumor environments. Nevertheless, little is known about the potential role of mitophagy in MM, except that a previous study described cytotoxicity associated with increased mitophagy in bortezomib-resistant myeloma cells.<sup>11</sup> However, additional evidence supporting this result is insufficient, implying that the effects of mitophagy on MM still require further investigation.

Homoharringtonine (HHT) is a natural alkaloid extracted from *Cephalotaxus* species that has been widely used to treat certain hematological diseases and malignancies, such as leukemia and myelodysplastic syndrome.<sup>12</sup> Accumulating evidence has confirmed that HHT also exerts antimyeloma effects on MM cells by inducing apoptosis.<sup>13,14</sup> For instance, HHT exerts cytotoxic effects on MM cells by inhibiting the Akt pathway and downregulating the expression of related downstream genes, including *nuclear kappa B*, *XIAP*, *cIAP* and *cyclin D1*,<sup>15</sup> which are crucial factors involved in disease progression and chemotherapy resistance. Considering the predominant function of mitophagy in tumor progression, in the present study, we assessed whether HHT exerts antimyeloma effects in vitro and in a xenograft model by regulating mitophagy to further substantiate the role of mitophagy in MM. These findings provide a new perspective for the treatment of MM.

## Materials and Methods

### Cell Viability

MM.1S, RPMI 8226 and H929 cells were obtained from the American Type Culture Collection (Manassas, VA, USA) and cultured without or with different concentrations of HHT for 12, 24, 48 or 72 h, and then the viability of the treated cells was measured with a Cell Counting Kit-8 (CCK-8) assay (Beyotime, Shanghai, China) according to the manufacturer's protocol. The optical density (OD) values were measured at 450 nm with a microplate reader (Thermo Fisher Scientific, Waltham, MA, USA).

### SCID Mouse Xenograft Model

The study protocols for the animal experiments were approved by the Committee of Research Animals of the Affiliated Hospital of Shandong University of Traditional Chinese Medicine. The procedures were performed in accordance with the Guidelines for the Care and Use of Laboratory Animals. A total of  $3 \times 10^7$ /mL MM.1S cells in 100  $\mu$ L of RPMI 1640 medium together with 100  $\mu$ L of Matrigel basement membrane matrix were subcutaneously injected into the right hypochondrium of male SCID mice aged 6–8 weeks. The tumor size was calculated with the formula  $V = 4\pi/3 \times R^3$ , where  $R = (\text{tumor length} + \text{tumor width})/2$ . The tumor length and width were measured every three days with a Vernier caliper and were accurate to 0.1 mm. Tumors were allowed to grow to a size greater than 100 mm<sup>3</sup>, and then the mice were randomly assigned to the control group and the HHT group ( $n=10$  mice/group). The HHT group was intravenously injected with 1 mg/kg HHT from days 1–5, whereas the control group was treated with the same volume of normal saline. Following HHT administration, the tumors were harvested, photographed and immunohistochemically stained. Hematoxylin-eosin (HE) staining and immunohistochemistry (IHC) staining for Beclin 1 and Parkin were performed using standard protocols to assess the number of tumor cells and the level of mitophagy.<sup>16</sup>

### Immunofluorescence Staining for Autophagosomes

Cells were fixed with paraformaldehyde for 15 min, permeabilized with 0.1% Triton X-100, washed three times with 0.5% Triton X-100 in PBS, and stained with an anti-light chain 3B (LC3B) antibody (Bioswamp, MAB43969) to assess autophagosome puncta in the cytoplasm. Then, the cells were incubated with an Alexa Fluor 488-conjugated AffiniPure goat

anti-rabbit antibody (Bioswamp, SAB43742) in the dark for 2 h. Both the primary and secondary antibodies were diluted in PBS containing 0.5% Triton X-100. After the cells were mounted on glass slides with DAPI-containing antifade sealant (Bioswamp), fluorescence images were captured directly using a fluorescence microscope (Leica, Wetzlar, Hesse-Darmstadt, Germany).

## Evaluation of the mtDNA Copy Number

The relative mtDNA copy number was determined using qPCR with primers for the mitochondrial 16S rRNA gene. Fold-changes were calculated using the  $\Delta\Delta C_t$  method with normalization to ACTB. All PCR reactions were performed in triplicate. Primers for the 16S rRNA were: 5'-GGTGCAGCCGCTATTAAAGG-3' (forward) and 5'-ATCATTTACGGGGGAAGGCG-3' (reverse). Primers for the ACTB rRNA were: 5'-TGACGTGGACATCCGCAAAG-3' (forward) and 5'-CTGGAAGGTGGACAGCGAGG-3' (reverse).

## Evaluation of Mitochondrial Function

The mitochondrial membrane potential (MMP) was evaluated with a Mitochondrial Membrane Potential Detection Kit (Bioswamp). The treated cells were incubated with the JC-1 staining solution for 20 min at RT and then washed twice with PBS. Fluorescence was measured using a flow cytometer.

The monoamine oxidase (MAO) activity, cytochrome c oxidase (COX) level and the function of the mitochondrial outer membrane were estimated using a monoamine oxidase activity colorimetric assay kit (GMS50022.1), purified mitochondrial cytochrome c oxidase activity assay kit (GMS10014.2) and mitochondrial outer membrane function testing kit (GMS10014.1) according to the manufacturer's protocols. All these assay kits were purchased from GenMed (Shanghai, China).

## MitoTracker Green FM Staining

Cells were washed with PBS and then incubated with 400 nM MitoTracker Green FM (Molecular Probes) for 30 min at RT to detect the mitochondrial morphology. Then, the cells were washed twice with PBS and the structure of the mitochondria was observed using an inverted fluorescence microscope.

## Analysis of the Colocalization of Mitochondria with Mitophagy Markers

The colocalization of mitochondria with LC3 puncta, lysosome and Parkin were observed using confocal

fluorescence microscopy. MM.1S cells were transfected with a mixture of 2  $\mu$ g of the GFP-LC3 plasmid (Addgene, #22405) and 5  $\mu$ L of Cell Light<sup>TM</sup> Mitochondria-RFP (Thermo Fisher Scientific, C10505) to explore the colocalization of mitochondria and autophagosomes. The medium was changed after 12 h and the cells were cultured for 24 h. After a 12 h treatment with HHT, the colocalization of LC3 puncta with mitochondria was examined using a laser scanning confocal microscope. MM.1S cells were treated with or without HHT (25 ng/mL) for 24 h, followed by a wash with PBS to detect the colocalization of mitochondria and lysosomes. Then the cells were stained with MitoTracker Green (Thermo Fisher Scientific, M7514), which was diluted with fresh medium to a final concentration of 200 nM. After 30 min, LysoTracker Red (Thermo Fisher Scientific, L-7528) was added at a final concentration of 25 nM and the cells were stained for another 10 min before imaging. Yellow puncta that were detected with the confocal microscope in 30 cells of each group were quantified, which represented the colocalization of mitochondria with autophagosomes or lysosomes. Cells were cultivated on cell slides for staining to evaluate the colocalization of mitochondria with Parkin. MitoTracker<sup>TM</sup> Red CMXRos (Thermo Fisher Scientific, M7512) (500 nM) was added to living cells at 37 °C for 30 min to label the mitochondria, and then cells were fixed with 4% PFA. Cells were permeabilized with 0.1% TritonX-100 for 5 min at RT. The cell slides were incubated with Parkin antibodies (1:100) at 4 °C overnight. After the incubation with the secondary antibody, cells were imaged with a fluorescence microscope at a wavelength of 550 nm for MitoTracker<sup>TM</sup> Red CMXRos and the appropriate wavelengths for fluorophore-conjugated secondary antibodies. For quantification, 10 fields were randomly selected from each group, and the number of cells per 0.25 mm<sup>2</sup> was evaluated. The intensity of immunofluorescence staining was analyzed using Image J software.

## Western Blotting (WB) Analysis

Treated cells were lysed with RIPA lysis buffer (Bioswamp), and the protein concentrations in the lysates were measured with a BCA protein assay kit (Bioswamp). Equal amounts of proteins in each sample were loaded onto gels and subjected to SDS-PAGE. The separated proteins on the gels were then transferred to nitrocellulose membranes. Each immunoblot was blocked with 5% nonfat milk in TBST for 2 h prior to an

overnight incubation at 4 °C with specific antibodies. The following primary antibodies were used for Western blotting: Bcl-2 (Proteintech, 60178-1-Ig), Bax (Proteintech, 50599-2-Ig), cleaved caspase-3 (Cell Signaling Technology, 9664), LC3B (Bioswamp, MAB43969), Beclin 1 (Proteintech, 66665-1-Ig), Parkin (Proteintech, 14060-1-AP), P62 (Proteintech, 18420-1-AP), Tim23 (Proteintech, 11123-1-AP), CoxIV (Cell Signaling Technology, 4844) and NDP52 (Cell Signaling Technology, 60732). The blots were washed with TBST three times for 15 min each and then incubated with secondary antibodies for 2 h at RT. Finally, enhanced chemiluminescence reagent was used to visualize the bands, and the intensities were determined to further evaluate the levels of each protein.

## Transmission Electron Microscopy (TEM)

Mitophagic vesicles and mitochondrial morphology were observed using TEM (Hitachi, HT7700). Treated cells were fixed with 2.5% glutaraldehyde and sodium pyruvate for 24 h, postfixed with 2% OsO<sub>4</sub> for 2 h, and then dehydrated. The fixed samples were subsequently cut into thin sections (60 nm) with a diamond knife and stained with uranyl acetate for 20 min and lead citrate for 15 min. After the samples were washed and dried, images were obtained using TEM.

## RNA Interference (RNAi)

Prior to treatment, some cells were transfected with a short hairpin RNA (shRNA) targeting *Parkin* (Santa Cruz, sc-42158) or with a nonsilencing scrambled (sc) control shRNA (Santa Cruz, sc-108080) for 48 h using Lipofectamine 3000 transfection reagent as described in a previously reported protocol.<sup>17</sup> Cells were collected, and Parkin levels were detected using WB analysis to evaluate the transfection efficiency.

## Statistical Analysis

The data are presented as the mean  $\pm$  standard deviation (SD) of three independent experiments. SPSS Statistics 26.0 software was used for the analyses. One-way analysis of variance was used to assess statistical significance; Student's *t*-test was used for comparisons between two groups. A *P*-value  $\leq$  0.05 was considered to indicate a statistically significant difference.

## Results

### HHT Inhibited Proliferation and Promoted Mitophagy in MM Cell Lines

The CCK8 assay was performed to measure the 50% inhibitory concentration (IC<sub>50</sub>) of HHT in MM cells. The viability of MM.1S, RPMI8226 and H929 cells was detected after treatment with 3.125, 6.25, 12.5, 25 and 50 ng/mL HHT for 12, 24, 48 or 72 h. As shown in Figure 1A–C, HHT dramatically reduced the cell viability in a dose- and time-dependent manner. The IC<sub>50</sub> values recorded at 48 h in MM.1S, RPMI8226 and H929 cells were 23.09 $\pm$ 1.20 ng/mL, 19.11 $\pm$ 1.53 ng/mL and 33.75 $\pm$ 9.68 ng/mL, respectively (Figure 1D), suggesting that HHT exhibited potent cytotoxicity toward MM cells.

Subsequently, based on the IC<sub>50</sub> of HHT, we further determined whether the process of mitophagy is involved in the antiproliferative effect of HHT on MM cells. We evaluated the levels of mitophagy-associated proteins, including LC3B, Beclin 1, P62, Pink 1 and Parkin using WB. Autophagosome formation is a vital stage of mitophagy, and LC3 is a ubiquitin-like protein that is responsible for the recruitment of lipid molecules to elongate the autophagosome membrane.<sup>18,19</sup> The conversion of LC3-I to LC3-II reflects the number of autophagosomes to some extent.<sup>20</sup> As shown in Figure 1E–H, the ratio of LC3-II/LC3-I was significantly increased in the HHT groups compared with the negative control group after treatment for 48 h (all *P*<0.01). Moreover, P62, also named sequestosome 1 (SQSTM1), is a well-known autophagy receptor that is constantly degraded through interactions with LC3;<sup>21</sup> it also participates in the Pink 1/Parkin mitophagy pathway by interacting with Parkin.<sup>22</sup> Notably, P62 accumulates when mitophagy is inhibited. Treatment at 25ng/mL HHT markedly reduced the level of the P62 protein compared to other groups (Figure 1E–H, *P*<0.01), indicating an increase in mitophagic flux in MM cells stimulated with HHT. Beclin 1 is an autophagy effector protein that contributes to the initiation of mitophagy,<sup>23</sup> and the HHT treatment groups exhibited increased levels of Beclin 1 (Figure 1E–H), but the effect of 25ng/mL HHT was more notable than the effect of 12.5ng/mL HHT. In addition, compared with the control group, HHT induced a substantial accumulation of Pink 1 and Parkin, which are predominant factors involved in the initiation of mitophagy in MM cells (Figure 1E–H). Overall, HHT treatment significantly decreased the survival of MM cells and



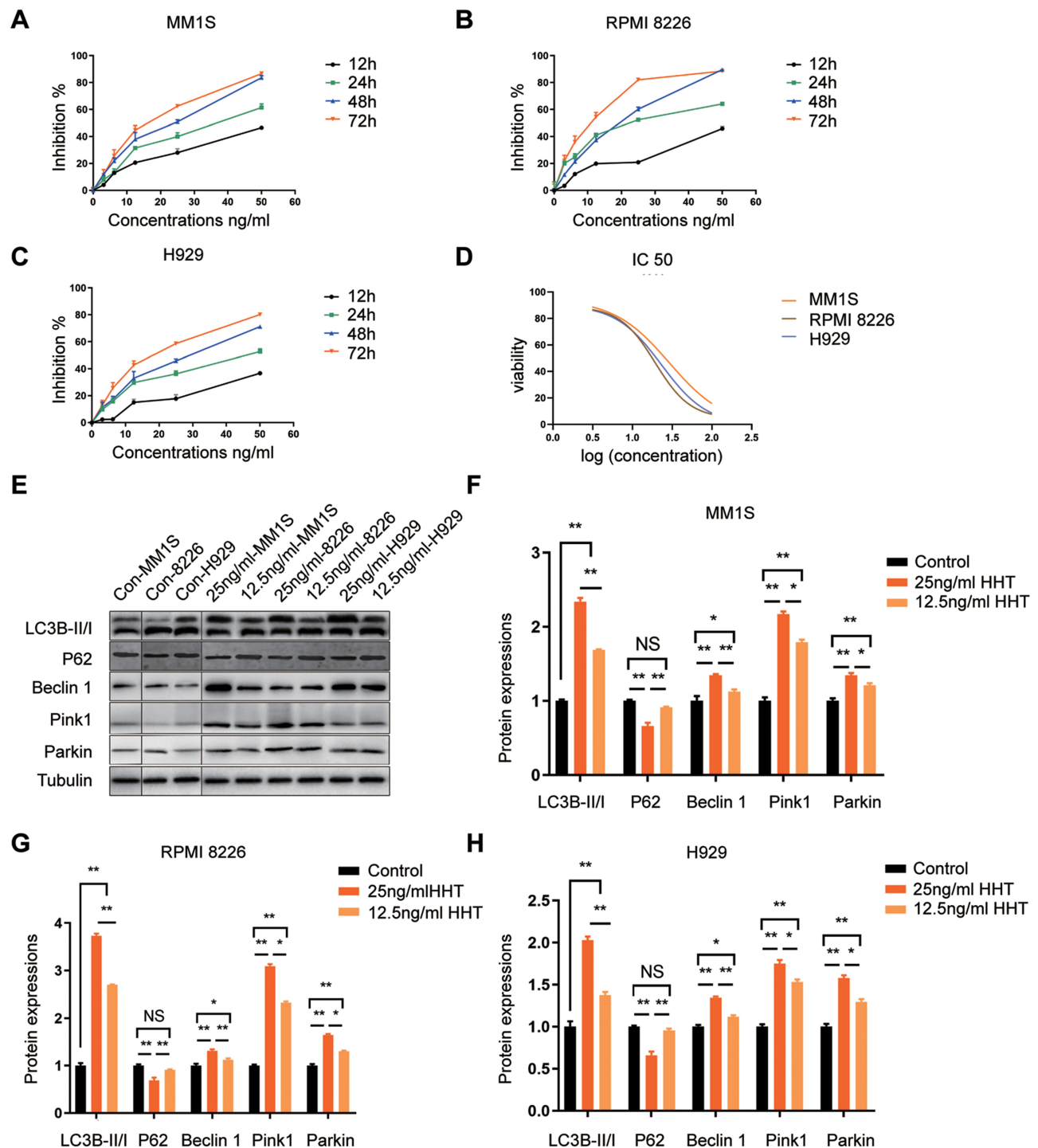


**Figure 1** HHT inhibited the proliferation of MM.1S, RPMI 8226 and H929 cells and promoted mitophagy. Cells were treated with different concentrations (0, 3.125, 6.25, 25 and 50 ng/mL) of HHT for 12, 24, 48 and 72 h. HHT inhibited the proliferation of MM cells in a dose- and time-dependent manner. (A) HHT inhibited the proliferation of MM.1S cells. (B) HHT inhibited the proliferation of RPMI 8226 cells. (C) HHT inhibited the proliferation of H929 cells. (D) The IC<sub>50</sub> was calculated at 48 h after the assessment of cell viability using the CCK-8 assay. (E) Levels of the LC3, P62, Beclin I, Pink I and Parkin proteins were evaluated by Western blot after cells were treated with 25ng/mL or 12.5 ng/mL HHT for 48 h. HHT promoted mitophagy in MM cells, as evidenced by the increased LC3-II/LC3-I ratio, Beclin I and Parkin levels and a decreased P62 level. Levels of LC3, P62, Beclin I, Pink I and Parkin in MM.1S cells (F), RPMI 8226 cells (G) and H929 cells (H) are shown. Each experiment was repeated three times. The data are presented as means±SD. Every experiment was repeated in triplicate. One-way ANOVA was used to assess statistical significance. \**P*<0.05, \*\**P*<0.01, and NS *P*>0.05 compared to the control.

increased the level of mitophagy related factors, implying that HHT might reduce MM cell viability by inducing mitophagy.

## HHT Exerted Potent Antitumor and Pro-Mitophagy Effects on an MM Xenograft Model

We established an MM xenograft model through the subcutaneous injection of MM.1S cells to further verify the antimyeloma effect of HHT in vivo and characterize the role of mitophagy in the process. Compared to the

model group, the HHT-treatment group displayed prolonged survival (Figure 2A,  $P < 0.05$ ). Moreover, as shown in Figure 2B, the tumor volume of the treated group was significantly smaller than the control group ( $P < 0.01$ ), implying that HHT efficiently suppressed tumor growth. In addition, according to the results of HE staining, the tumor cells in each group were arranged diffusely in sheets, with a large number of densely packed plasmablasts and proplasmacytes. Compared with the model group, which presented 72 mitotic figures/10 high-power fields (HPFs), the HHT group exhibited a significantly reduced number of mitotic figures of

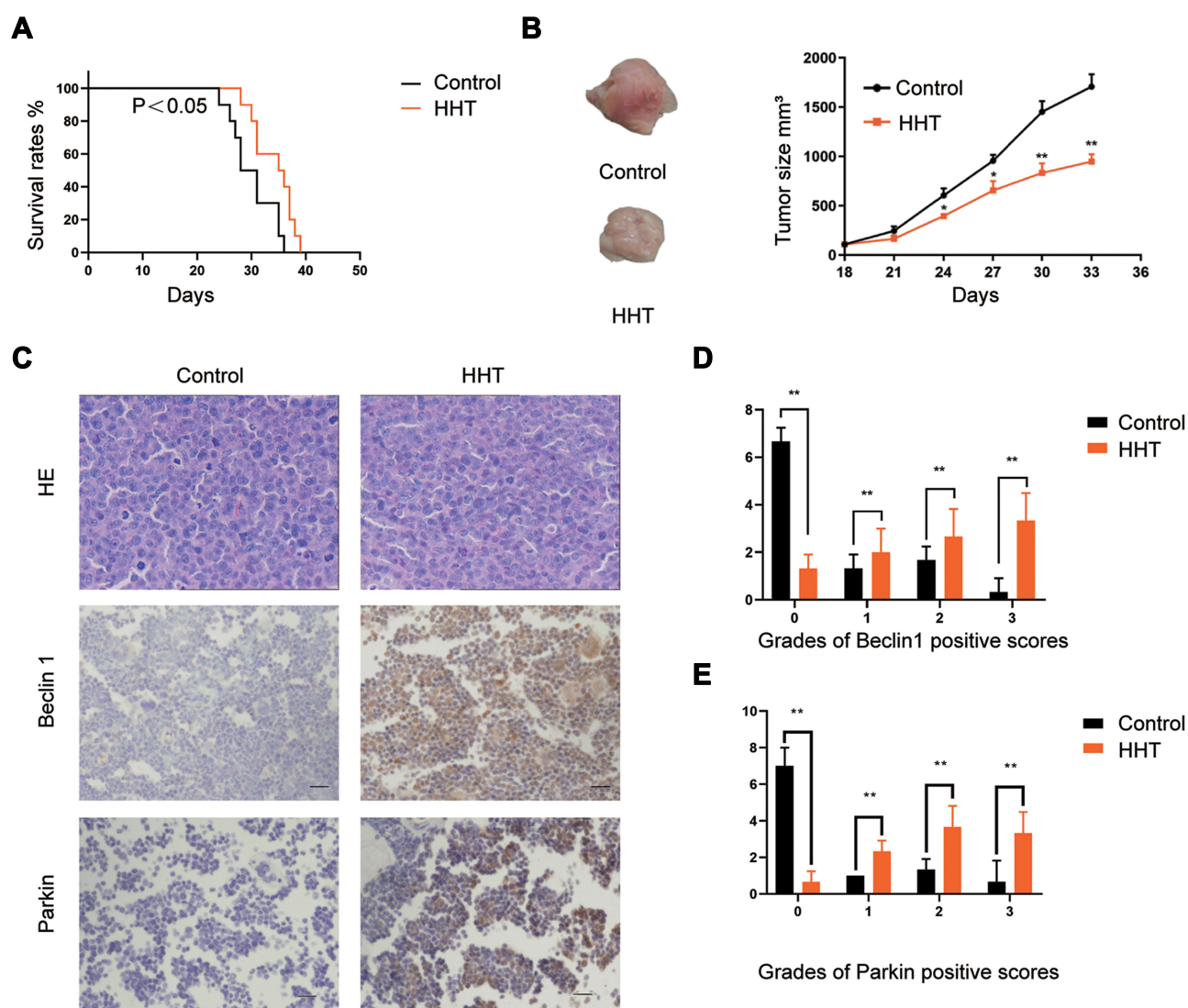


**Figure 2** HHT exerted an antitumor effect and enhanced mitophagy in the MM xenograft model. Male SCID mice (6–8 weeks) were subcutaneously injected with 100  $\mu$ L of  $3 \times 10^6$ /mL MM.1S cells to establish an MM xenograft model and then treated with or without HHT. (A) Compared with the untreated group, the HHT treatment significantly prolonged survival. (B) The HHT treatment suppressed tumor growth, resulting in a reduced tumor size. As shown in the photograph, the length and width of the tumor in the control group was 8.1 mm and 7 mm, respectively, whereas the length and width were 6.3 mm and 5.4 mm, respectively, in the HHT group. (C) HE staining of the excised tumors from the model group and HHT group. (D) IHC of Beclin 1 in the model group and HHT group. (E) IHC staining for Parkin in the model group and HHT group. The data are presented as means  $\pm$  SD. Every experiment was repeated in triplicate. Student's t-test was used to compare the data between two groups. \* $P < 0.05$ , \*\* $P < 0.01$ , and NS  $P > 0.05$  compared to the control.

approximately 35/10 HPFs (Figure 2C), indicating that HHT exerted a potent tumoricidal effect and alleviated the progression of MM. We performed IHC staining for Beclin 1 and Parkin to determine whether Parkin-mediated mitophagy was activated in the xenograft model. As expected, Beclin 1 and Parkin were expressed at higher levels in the HHT group than in the model group (Figure 2D and E,  $P < 0.01$ ). Consistent with the results of the in vitro experiments, the in vivo studies revealed that HHT exerts an antimyeloma effect, and the induction of mitophagy correlates with the tumoricidal mechanism.

## HHT Induced Mitochondrial Damage by Promoting Excess Parkin-Mediated Mitophagy

Since we established a link between mitophagy and the potency of HHT, we treated MM.1S cells with rapamycin (Rap) and hydroxychloroquine (Hcq) in combination with HHT and investigated the level of mitophagy by detecting the levels of mitochondria-related indicators to further identify the pro-mitophagy effect of HHT. As shown in Figure 3A, the intensity of GFP-LC3 fluorescence was increased in the HHT group and the group treated with HHT combined with Rap compared to the other groups; the number of LC3-positive cells in HHT-treated groups was remarkably increased compared with the control group ( $P < 0.01$ ). Moreover, the number of mitochondria number was decreased when mitophagy occurred. As presented in Figure 3B, the relative number of mitochondria was significantly decreased in MM.1S cells treated with HHT or HHT plus Rap compared with the control group and HHT plus Hcq group ( $P < 0.01$ ). A similar trend was observed for the intensity of the MitoTracker Green probe (Figure 3C). Compared with the control group, the HHT group and HHT plus Rap group exhibited a decreased number of mitochondria ( $P < 0.01$ ), whereas the HHT plus Hcq treatment did not exert a noticeable effect on the number of mitochondria.

The characteristic mitochondrial morphology was observed using TEM. Compared with the other groups, the HHT group exhibited the most severe mitochondrial swelling and rupture along with structural damage and increased numbers of vacuoles (Figure 3D). Hcq notably alleviated mitochondrial dysfunction in the HHT-treated group, while no significant alleviation was detected in the HHT plus Rap-treated group.

Subsequently, we further examined whether HHT, along with Rap or Hcq, affected mitochondrial function at the molecular level. Consistent with the findings described above, the HHT group showed a reduction in the levels of the mitochondrial proteins Tim23 and CoxIV compared to the other groups (Figure 3E). Combined treatment with HHT and Rap also resulted in a substantial decrease in the levels of these two proteins. In contrast, significantly higher Tim23 and CoxIV levels were observed in the control group and HHT plus Hcq group ( $P < 0.01$ ), suggesting that intracellular mitochondria were severely damaged due to the mitophagy-promoting effect of HHT or HHT plus Rap. In addition, compared to the control and HHT plus Hcq groups, the HHT group exhibited a marked decrease in the Bcl-2/Bax ratio (Figure 3E,  $P < 0.01$ ). However, a significant difference was not observed between the HHT group and the HHT plus Rap group ( $P > 0.05$ ). Since Bcl-2 proteins inhibit mitophagy by blocking the translocation of Parkin to depolarized mitochondria while Bax destabilizes the mitochondrial membrane and increases mitophagy,<sup>24–26</sup> these results imply that HHT strikingly increases mitophagy.

Parkin is widely recognized as a vital mediator of mitophagy.<sup>27</sup> Additionally, the cargo receptor NDP52 has recently been shown to be required for Parkin-dependent mitophagy by interacting with the FIP200/ULK1 complex.<sup>28</sup> We examined the levels of Parkin and NDP52 in the MM.1S cells to further explore the mechanism by which the HHT treatment induces mitophagy. The level of Parkin was significantly increased by HHT; however, this increase was attenuated by Hcq (Figure 3E), a similar trend in the NDP52 levels was also observed. Moreover, we examined levels of the Parkin and NDP52 proteins on isolated mitochondria, and more Parkin and NDP52 accumulated on the mitochondria after treatment with HHT or HHT plus Rap compared with the other two treatments (Figure 3F), underscoring that HHT initiated mitophagy. Moreover, we examined cleaved caspase 3 levels in MM.1S cells to determine whether the antimyeloma effect of HHT was mediated by the induction of apoptosis. The HHT and HHT plus Rap group presented low levels of the cleaved caspase 3 protein, indicating that HHT-induced mitophagy was not associated with the priming of apoptosis. Furthermore, a significant difference in the Bax levels in the isolated mitochondria was not observed among the 4 groups, confirming that HHT did not lead to the translocation of Bax on mitochondria and did not induce Bax-dependent apoptosis, suggesting that

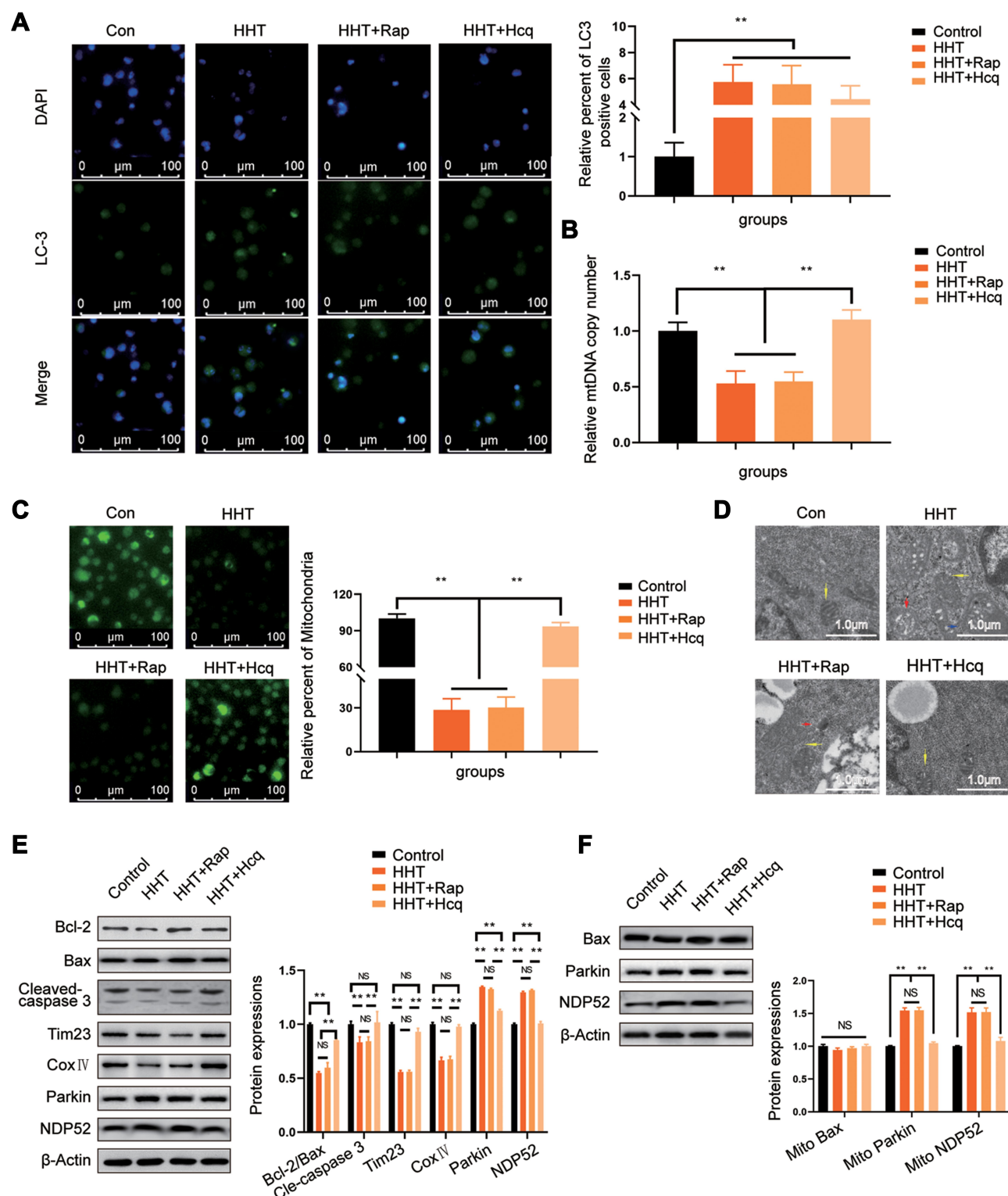


**Figure 3** HHT induced excess mitophagy and mitochondrial damage in MM.1S cells. MM.1S cells were treated with 25ng/mL HHT alone or in combination with Rap or Hcq for 48 h. **(A)** The fluorescence intensity was evaluated using fluorescence microscopy; the green color indicates LC3, and DAPI was used to stain the nuclei. HHT increased the LC3 fluorescence intensity to the greatest extent. **(B)** Quantification of the mtDNA copy number in different groups. **(C)** Mitochondrial fluorescence (green) was monitored using fluorescence microscopy. **(D)** Representative TEM images of the morphology of MM.1S cells treated with HHT alone or in combination with Rap or Hcq. The HHT group showed the most severe mitochondrial swelling and cristae breakage, with large numbers of mitophagic vesicles. **(E)** WB analysis of the levels of Bcl-2, Bax, cleaved caspase 3, Tim 23, CoxIV, Parkin, NDP52 and actin protein expression in MM.1S cells. **(F)** WB analysis of levels of the Bax, Parkin, NDP52 and actin proteins in the isolated mitochondria. The data are presented as means $\pm$ SD. Every experiment was repeated in triplicate. One-way ANOVA was used to assess statistical significance. \*\* $P < 0.01$ , and NS  $P > 0.05$  between the indicated pairs of groups.



the antimyeloma effect of HHT was likely dependent on the potent pro-mitophagy effect rather than the induction of apoptosis. Overall, the addition of Rap did not produce a significant synergistic effect with HHT on the number of mitochondria, the reduction in the levels of mitochondrial proteins or the increase in Parkin and NDP52 levels, indicating that the HHT treatment induced the mitophagy at the ceiling threshold. A moderate level of mitophagy exerts a pro-survival role on cells, whereas excess mitophagy beyond the ceiling mitophagy threshold results in a death due to the uncontrollable degradation of vital cellular components.<sup>29</sup> In summary, HHT disrupts the quantity and quality of mitochondria by promoting excess Parkin-mediated mitophagy.

### HHT Induced Mitochondrial Colocalization with Mitophagy Markers and Mitochondrial Dysfunction

The colocalization of mitochondria (labelled with MitoTracker Red) and LC3 puncta (labeled with RFP LC3 Green) was observed using a confocal fluorescence microscope to further confirm the pro-mitophagy effect of HHT. Compared with the control group, each HHT-treated cells contained more mitochondria-localized LC3 puncta (Figure 4A,  $P<0.01$ ). Moreover, HHT conspicuously increased the colocalization of lysosomes (labeled with LysoTracker Red) with mitochondria (labeled with MitoTracker Green) (Figure 4B). A greater number of mitochondria-localized lysosomes in each cells was quantified in the HHT group (Figure 4B,  $P<0.01$ ). Moreover, increased colocalization of mitochondria (labeled with MitoTracker Red) with Parkin (Green) was observed in the HHT group (Figure 4C,  $P<0.01$ ), which further confirmed that HHT triggered Parkin-mediated mitophagy. The activity of mitochondrial enzymes, including monoamine oxidase (MAO) and cytochrome c oxidase (COX), and mitochondrial outer membrane function were detected to determine whether HHT-induced mitophagy was related to mitochondrial function. According to previous studies, MAO is located in the outer membrane of mitochondria, and its activation plays a crucial role in facilitating mitochondrial dysfunction.<sup>30</sup> COX is located in the inner membrane and is part of the electron transport chain. Observations of COX activity are straightforward methods to evaluate mitochondrial dysfunction.<sup>31</sup> Compared with the control group, MM.1S cells exposed to HHT for 12, 24 and 72 h exhibited evident increases in MAO activity and

damage to the mitochondrial outer membrane and a decrease in the COX level, suggesting that HHT-induced mitophagy can cause substantial mitochondrial damage (Figure 4D–F,  $P<0.01$ ).

### Knockdown of Parkin Reduced the Susceptibility of Cells to HHT-Induced Mitophagy and Death

We constructed an shRNA targeting *Parkin* to test the hypothesis that the antimyeloma effect of HHT depends on induction of excess Parkin-mediated mitophagy. All cells were transfected with either the scrambled shRNA or *Parkin*-shRNA, treated with or without HHT, and a WB analysis was performed to evaluate the levels of the Parkin protein. The viability of MM.1S cells was subsequently detected after transfection to identify the critical role of Parkin in the antimyeloma effect of HHT. As anticipated, compared to the control groups, the proliferation of the scrambled shRNA-transfected HHT group (scramble-HHT group) of MM.1S cells was reduced, a change that was abrogated by the knockdown of *Parkin* (Figure 5A,  $P<0.01$ ).

Mitophagy levels were assessed again to determine whether *Parkin* knockdown reversed the cytotoxic effects by reducing mitophagy and restoring mitochondrial function. As shown in the Figure 4B, fewer GFP-LC3 puncta were detected in the control groups than in the scramble-HHT group due to a basal level of mitophagy in MM.1S cells. Compared to the *Parkin*-shRNA-transfected HHT group (*Parkin*-shRNA-HHT group), the scramble-HHT group exhibited more intense GFP-LC3 fluorescence, implying that the *Parkin* deficiency substantially impaired mitophagy flux (Figure 5B). Moreover, the scramble-HHT group displayed the most severe impairments in the MMP and mitochondrial ultrastructure (Figure 5C and D). Surprisingly, the MMP level in the *Parkin*-shRNA-HHT group was also significantly lower than the control groups (Figure 5C,  $P<0.01$ ), suggesting that HHT might exert other toxic effects on mitochondria that contribute to the mitochondrial dysfunction apart from excess Parkin-mediated mitophagy. In addition, the scramble-HHT group was confirmed to exhibit excess mitophagy and the substantial destruction of mitochondria, as evidenced by the increase in the LC3-II/LC3-I ratio and decreases in the Bcl-2/Bax ratio and Tim23 and CoxIV levels (Figure 5E,  $P<0.01$ ), while little perceptible change was observed in the *Parkin*-shRNA-HHT group compared to

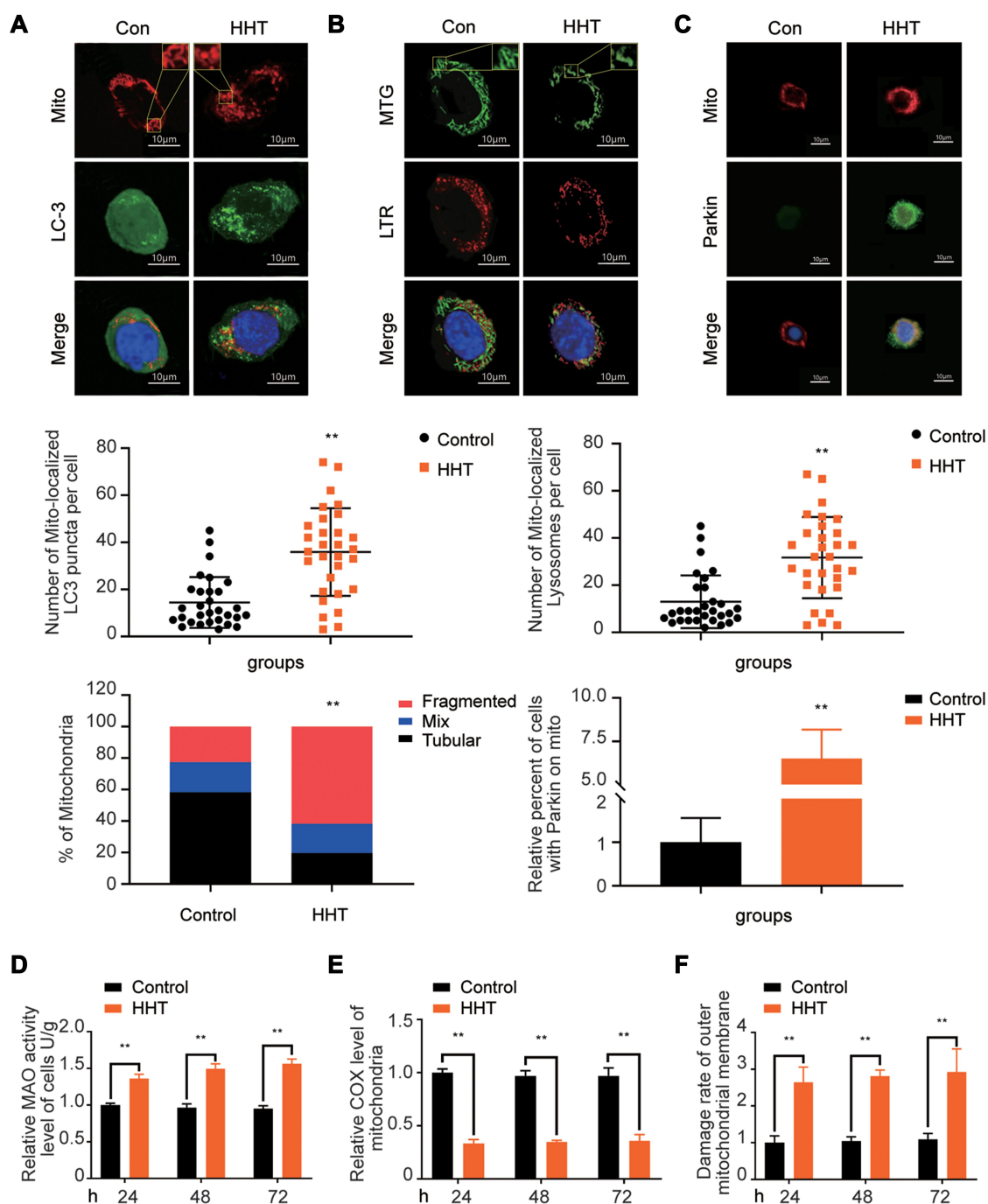


**Figure 4** The HHT treatment triggered mitophagy and impaired mitochondrial function. MM.IS cells were treated with or without 25ng/mL HHT for 24 h. Confocal fluorescence microscopy was used to observe the colocalization of mitochondria with autophagosomes, lysosomes and Parkin. **(A)** The colocalization of mitochondria and LC3 puncta; red, MitoTracker Red; green, GFP-LC3; gold, merge. The gold puncta were considered autophagosomes containing mitochondria and were quantified. The average number of mitochondria-localized LC3 puncta per cell was quantified. **(B)** The colocalization of mitochondria and lysosomes; green, MitoTracker Green; red, LysoTracker Red; gold, merge. The average number of mitochondria-localized lysosomes per cell was quantified. **(C)** The colocalization of mitochondria and Parkin; red, MitoTracker Red; green, Parkin; gold, merge. The relative percentage of cells with Parkin on mitochondria were counted. **(D)** Relative MAO activity in MM.IS cells treated with or without HHT (25ng/mL) for 24, 48 or 72 h. **(E)** Relative COX levels of mitochondria treated with or without HHT (25ng/mL) for 24, 48 and 72 h. **(F)** The rate of damage to the mitochondrial outer mitochondrial membrane of MM.IS cells was evaluated after treatment with or without HHT (25ng/mL) for 24, 48 or 72 h. Every experiment was repeated in triplicate. Student's *t*-test was used to compare the data between two groups. \*\**P*<0.01, and NS *P*>0.05 between the indicated pairs of groups.

the control groups. Hence, we concluded that the antimyeloma effect of HHT is mediated by enhanced Parkin-dependent mitophagy and mitochondrial dysfunction.

## Discussion

Based on accumulating evidence, HHT potentially exerts antimyeloma effects; however, little is known about its

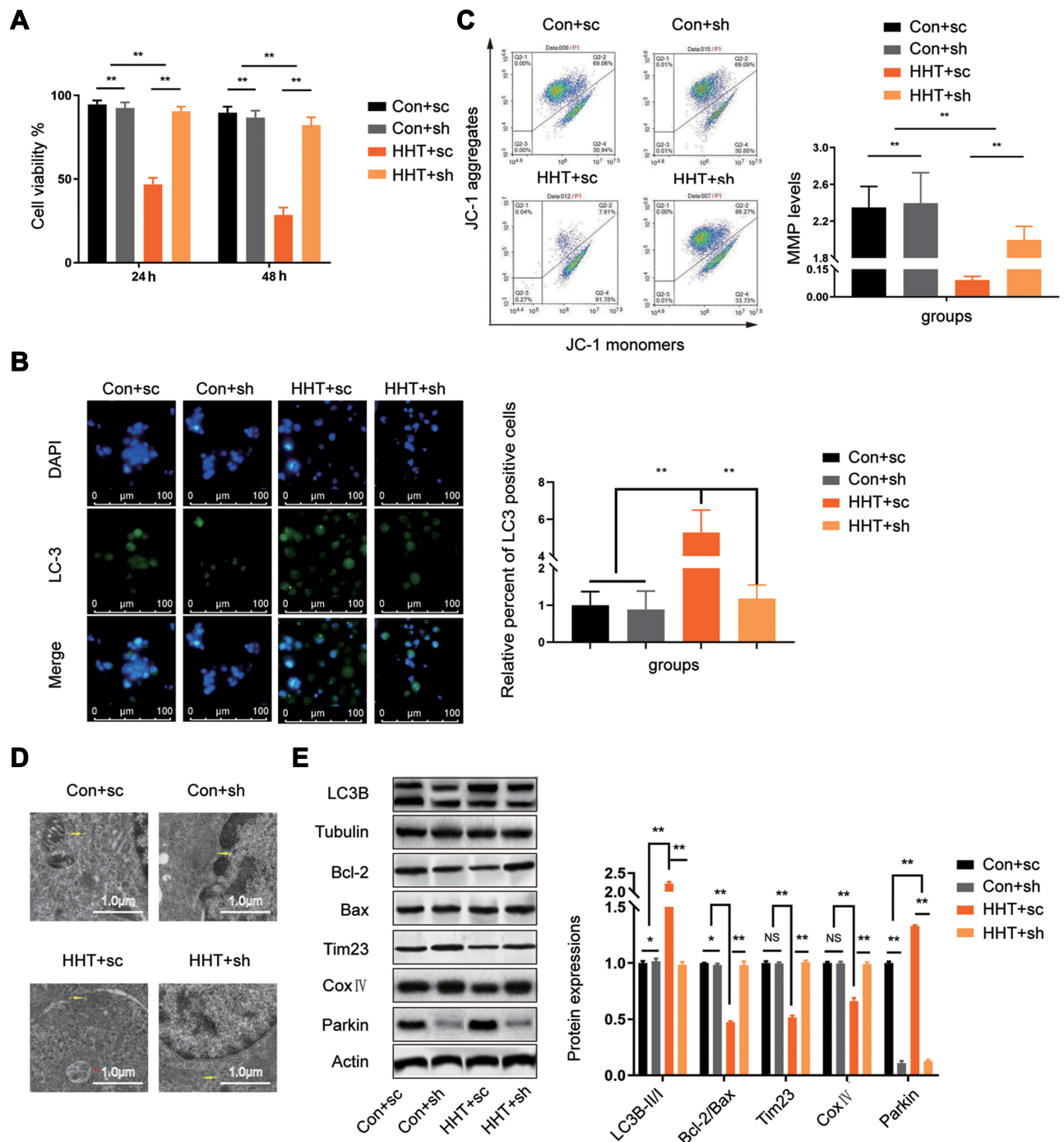


**Figure 5** *Parkin* knockdown reduced the ability of HHT to inhibit cell viability and promote mitophagy. All cells were transfected with the scrambled shRNA or *Parkin*-shRNA, and treated with or without 25ng/mL HHT. (A) Knockdown of *Parkin* reversed the substantial increase in cell death induced by HHT. (B) The fluorescence intensity of LC3 was evaluated; the green color indicates LC3, and DAPI was used to stain the nuclei. (C) The MMP was assessed using a mitochondrial membrane potential detection kit. The scramble-HHT group exhibited the lowest level of MMP. (D) Mitochondrial ultrastructure was detected using TEM. The scramble-HHT group showed the most severe mitochondrial damage and massive mitophagic vesicles. (E) WB analysis of levels of LC3-II/LC3-I, Bcl-2, Bax, Tim 23, Cox IV, Parkin and actin (or tubulin) was performed. Each experiment was repeated three times. The data are presented as means $\pm$ SD. Every experiment was repeated in triplicate. One-way ANOVA analysis was used to assess statistical significance. \* $P$ <0.05, \*\* $P$ <0.01, and NS  $P$ >0.05 between the indicated pairs of groups.

role in promoting mitophagy in MM. To our knowledge, this study is the first to elucidate the mechanism underlying the effect of the HHT treatment on MM from the perspective of inducing excess mitophagy and regulating mitochondrial function, vital processes by which HHT exerts its tumoricidal effects on MM. Based on the results of the in vitro and in vivo experiments, HHT deregulates proliferation and inhibits tumor growth by inducing excess mitophagy and the accumulation of dysfunctional mitochondria.

HHT has consistently been shown to exert potential antitumor effects on MM.<sup>13–15</sup> Consistent with previous studies, HHT exposure inhibited the proliferation of MM.1S, RPMI8226 and H929 cells (Figure 1A–C), and the HHT treatment attenuated disease progression in an MM xenograft model by extending the survival time, decreasing the tumor size and decreasing the number of tumor cells in the present study (Figure 2).

The effect of mitophagy on cancer is controversial. On the one hand, mitophagy is considered a protective mechanism in cancer cells that blocks the initiation of the mitochondrial apoptosis cascade.<sup>7,32</sup> In addition, mitophagy provides a metabolic environment appropriate for tumorigenesis.<sup>33</sup> On the other hand, mitophagy has also been shown to induce mitophagic cell death, which has been well described in previous studies.<sup>29,34,35</sup> The Pink 1/Parkin signaling pathway is the most common pathway involved in mitophagy that triggers the translocation of the ubiquitin-binding receptor SQSTM1 or NDP52 to mitochondria to induce mitophagy.<sup>36</sup> In this study, the HHT-induced increase in mitophagy induced cell death (Figure 1) and inhibited tumor growth by increasing the levels of Beclin 1, Pink 1, Parkin and NDP52 (Figures 1 and 2). Parkin is a core factor in the conventional mitophagy pathway. In our study, *Parkin* deficiency resulted in low levels of mitophagy in HHT-treated MM.1S cells, with diminished GFP-LC3 fluorescence (Figure 5B) and reduced ratios of LC3-II to LC3-I and Bcl-2 to Bax (Figure 5E). The knock-down of *Parkin* also reduced the HHT-induced decrease in the expression of Tim23 and CoxIV (Figure 5E), and attenuated the HHT-induced impairments in the MMP and mitochondrial ultrastructure under TEM (Figure 5C and E), contributing to the alleviation of the HHT-induced mitochondrial damage. Moreover, *Parkin* knockdown reversed the inhibitory effect of HHT on MM cell proliferation (Figure 5A), further confirming that the antimyeloma potential of HHT depends on the induction of Parkin-mediated mitophagy and mitochondrial dysfunction. However, *Parkin*-shRNA transfection did not suppress mitophagy levels in control groups. In contrast,

compared to scrambled shRNA-transfected groups, *Parkin*-deficient MM.1S cells exhibited a higher ratio of LC3-II to LC3-I, a decreased ratio of Bcl-2 to Bax (Figure 5E,  $P<0.05$ ), and an increased MMP (Figure 5C,  $P<0.01$ ), potentially implying that basal mitophagy is a mechanism that protects mitochondria and *Parkin* knockdown triggered the other signaling pathway of mitophagy to maintain mitochondrial homeostasis and mitochondrial functions therefore causing the increase in the MMP. Nevertheless, the HHT-induced mitophagy promoted by HHT exceeded the basal levels, and thus the excess mitophagy disrupted mitochondrial function rather than preserving mitochondrial homeostasis.

In addition, treatment with the combination of HHT with Hcq, an autophagy inhibitor, attenuated the HHT-induced mitophagy caused by HHT alone (Figure 3). However, the addition of Rap, an autophagy inducer,<sup>37</sup> did not significantly enhance the HHT-induced mitophagy and mitochondrial dysfunction by HHT (Figure 3), suggesting that mitophagy homeostasis exists in MM cells and that HHT surpassed the threshold level.

Mitophagy is induced by oxidative stress and mitochondrial dysfunction. In turn, excess mitophagy is associated with mitochondrial dysfunction.<sup>38</sup> Excessive mitophagy contributes to the impairment of mitochondrial function, including changes in the MMP and mitochondrial mass, as well as the degradation of mitochondrial proteins,<sup>29</sup> which impairs the mitochondrial metabolic cycle.<sup>39</sup> We observed the colocalization of mitochondria with autophagosomes, lysosomes and Parkin, which indicated a high level of mitophagy (Figure 4A–C). Consistent with previous studies, we also observed increased MAO activity, increased damages to the mitochondrial outer membrane and substantial decreases in the levels of mitochondrial proteins and COX levels (Figures 3 and 4). In addition, the morphology and quantity of mitochondria were observed using fluorescence microscopy, and the HHT group showed a marked degradation of normal mitochondria (Figure 3C). TEM revealed that the HHT group exhibited the most severe mitochondrial swelling and rupture along with structural damage and increased numbers of vacuoles (Figure 3D). High metabolic levels are a hallmark of tumor progression, including myeloma progression.<sup>40</sup> Excess mitophagy induced by HHT decreases the number and percentage of mitochondria,<sup>41</sup> which accelerates MM cell death due to the lack of energy metabolism (Figure 6). Taken together, HHT



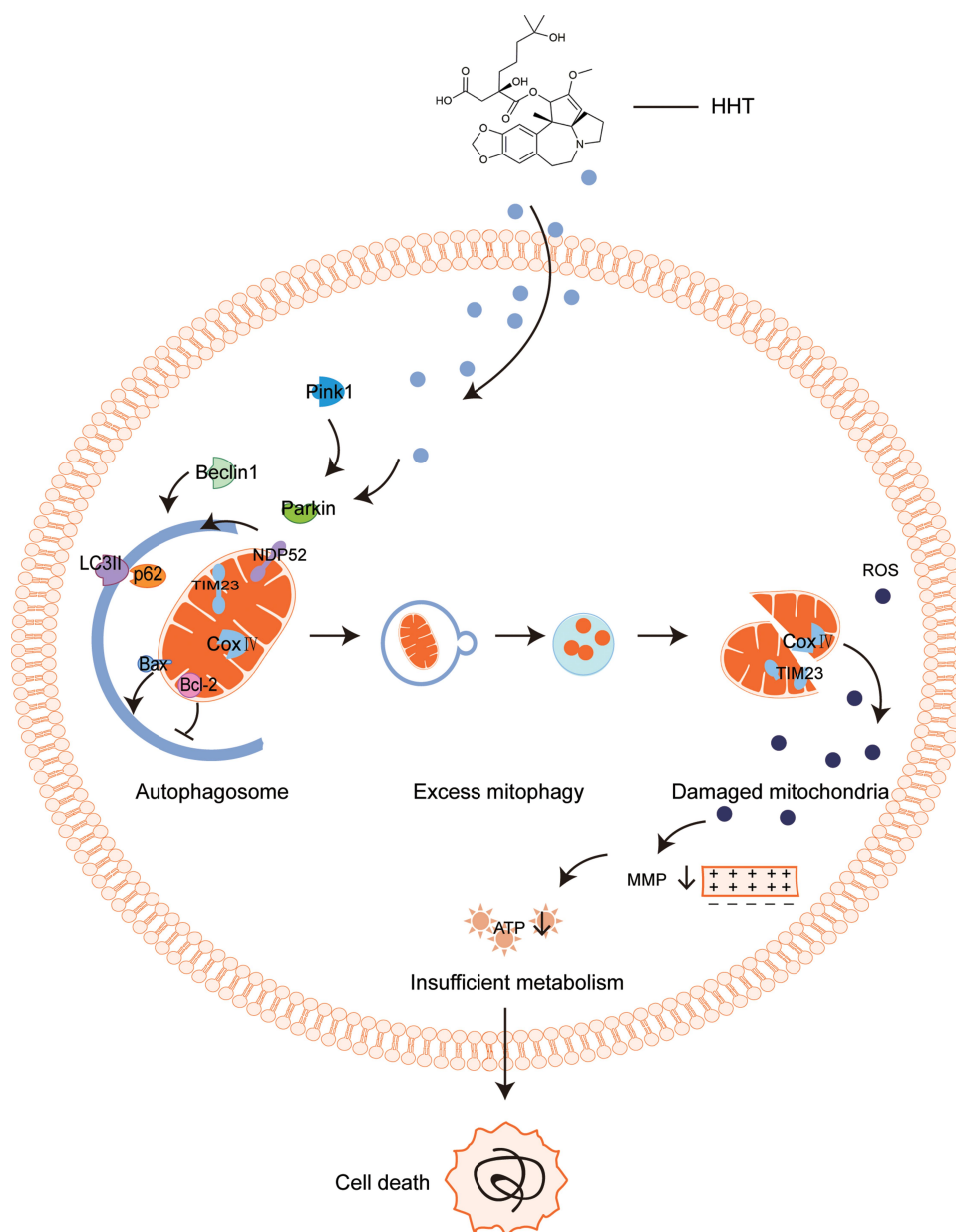


**Figure 6** Schematic of mechanism by which HHT exerts an antimyeloma effect through the induction of excess mitophagy. HHT induces excess mitophagy mediated by the Pink I/Parkin pathway, in which Beclin I and p62 are critical factors involved in the initial stage. NDP52 translocates to mitochondria to facilitate mitophagy. Bcl-2 inhibits the process, whereas Bax participates in promoting mitophagy. A large amount of LC3-I is recruited and converted into LC3-II to promote the formation of autophagosomes. As a result, excess mitophagy induces substantial mitochondrial damage, and dysfunctional and fractionated mitochondria accumulate leading to more severe mitochondrial destruction and insufficient metabolism that ultimately contribute to MM cell death.

substantially alters mitochondrial function and triggers MM cell death through lethal mitophagy.

Overall, the present study identified the antimyeloma effect of HHT and assessed whether mitophagy was involved in the mechanism. Recently, mitophagy modulation has been utilized as a target for the development of new therapeutic strategies for various cancers.<sup>6</sup> Based on our data, the natural extract HHT is a novel alternative drug that exerts anti-MM effects by inducing excess Parkin-mediated mitophagy.

Nevertheless, the present study undeniably has some limitations, as the downstream pro-death mechanism is unclear, which will be addressed in our next research project.

## Conclusions

In summary, HHT significantly reduces MM cell viability in vitro and suppresses tumor growth in a xenograft model. These effects are mediated by the induction of excess Parkin-mediated mitophagy and the dysregulation of

mitochondrial function. Based on our results, HHT is a promising treatment for MM, but further investigations are required.

## Ethical Approval

The study protocols for the animal experiments were approved by the Committee of Research Animals of the Affiliated Hospital of Shandong University of Traditional Chinese Medicine. The procedures were performed in accordance with the Guidelines for the Care and Use of Laboratory Animals.

## Funding

The study was supported by the National Natural Science Foundation of China (No.81774080), the Taishan Scholar Program (No. tsqn201812145) and the Key Technology Research and Development Program of Shandong (No.2019GSF108162).

## Disclosure

The authors report no conflicts of interest related to this study.

## References

1. Rollig C, Knop S, Bornhauser M. Multiple myeloma. *Lancet*. 2015;385(9983):2197–2208. doi:10.1016/S0140-6736(14)60493-1
2. D'Agostino M, Boccadoro M, Smith EL. Novel immunotherapies for multiple myeloma. *Curr Hematol Malig Rep*. 2017;12(4):344–357. doi:10.1007/s11899-017-0397-7
3. Yu L, Chen Y, Toozé SA. Autophagy pathway: cellular and molecular mechanisms. *Autophagy*. 2018;14(2):207–215. doi:10.1080/15548627.2017.1378838
4. Dombi E, Mortiboys H, Poulton J. Modulating mitophagy in mitochondrial disease. *Curr Med Chem*. 2018;25(40):5597–5612. doi:10.2174/0929867324666170616101741
5. Maycotte P, Marin-Hernandez A, Goyri-Aguirre M, Anaya-Ruiz M, Reyes-Leyva J, Cortes-Hernandez P. Mitochondrial dynamics and cancer. *Tumour Biol*. 2017;39(5):1010428317698391. doi:10.1177/1010428317698391
6. Kulikov AV, Luchkina EA, Gogvadze V, Zhivotovsky B. Mitophagy: link to cancer development and therapy. *Biochem Biophys Res Commun*. 2017;482(3):432–439. doi:10.1016/j.bbrc.2016.10.088
7. Vara-Perez M, Felipe-Abrio B, Agostinis P. Mitophagy in cancer: a tale of adaptation. *Cells*. 2019;8(5):493. doi:10.3390/cells8050493
8. Panigrahi DP, Prahara PP, Bhol CS, et al. The emerging, multifaceted role of mitophagy in cancer and cancer therapeutics. *Semin Cancer Biol*. 2019.
9. Panda PK, Naik PP, Meher BR, et al. PUMA dependent mitophagy by Abrus agglutinin contributes to apoptosis through ceramide generation. *Biochim Biophys Acta Mol Cell Res*. 2018;1865(3):480–495. doi:10.1016/j.bbamcr.2017.12.002
10. Basit F, van Oppen LM, Schockel L, et al. Mitochondrial complex I inhibition triggers a mitophagy-dependent ROS increase leading to necroptosis and ferroptosis in melanoma cells. *Cell Death Dis*. 2017;8(3):e2716. doi:10.1038/cddis.2017.133
11. Zheng Z, Fan S, Zheng J, et al. Inhibition of thioredoxin activates mitophagy and overcomes adaptive bortezomib resistance in multiple myeloma. *J Hematol Oncol*. 2018;11(1):29. doi:10.1186/s13045-018-0575-7
12. Lu S, Wang J. Homoharringtonine and omacetaxine for myeloid hematological malignancies. *J Hematol Oncol*. 2014;7:2. doi:10.1186/1756-8722-7-2
13. Kuroda J, Kamitsuji Y, Kimura S, et al. Anti-myeloma effect of homoharringtonine with concomitant targeting of the myeloma-promoting molecules, Mcl-1, XIAP, and beta-catenin. *Int J Hematol*. 2008;87(5):507–515.
14. Lou YJ, Qian WB, Jin J. Homoharringtonine induces apoptosis and growth arrest in human myeloma cells. *Leuk Lymphoma*. 2007;48(7):1400–1406. doi:10.1080/10428190701411466
15. Meng H, Yang C, Jin J, Zhou Y, Qian W. Homoharringtonine inhibits the AKT pathway and induces in vitro and in vivo cytotoxicity in human multiple myeloma cells. *Leuk Lymphoma*. 2008;49(10):1954–1962. doi:10.1080/10428190802320368
16. Dawicki W, Allen KJH, Jiao R, et al. Daratumumab-(225)Actinium conjugate demonstrates greatly enhanced antitumor activity against experimental multiple myeloma tumors. *Oncotarget*. 2019;8(8):1607673. doi:10.1080/2162402X.2019.1607673
17. Gou H, Zhao M, Xu H, et al. CSFV induced mitochondrial fission and mitophagy to inhibit apoptosis. *Oncotarget*. 2017;8(24):39382–39400. doi:10.18632/oncotarget.17030
18. Kung CP, Budina A, Balaburski G, Bergenstock MK, Murphy M. Autophagy in tumor suppression and cancer therapy. *Crit Rev Eukaryot Gene Expr*. 2011;21(1):71–100. doi:10.1615/CritRevEukaryotGeneExpr.v21.i1.50
19. Youle RJ, Narendra DP. Mechanisms of mitophagy. *Nat Rev Mol Cell Biol*. 2011;12(1):9–14. doi:10.1038/nrm3028
20. Kimura S, Fujita N, Noda T, Yoshimori T. Monitoring autophagy in mammalian cultured cells through the dynamics of LC3. *Methods Enzymol*. 2009;452:1–12.
21. Schlafl AM, Berezowska S, Adams O, Langer R, Tschan MP. Reliable LC3 and p62 autophagy marker detection in formalin fixed paraffin embedded human tissue by immunohistochemistry. *Eur J Histochem*. 2015;59(2):2481. doi:10.4081/ejh.2015.2481
22. Liu H, Dai C, Fan Y, et al. From autophagy to mitophagy: the roles of P62 in neurodegenerative diseases. *J Bioenerg Biomembr*. 2017;49(5):413–422. doi:10.1007/s10863-017-9727-7
23. Sun Y, Yao X, Zhang QJ, et al. Beclin-1-dependent autophagy protects the heart during sepsis. *Circulation*. 2018;138(20):2247–2262.
24. Gross A, Katz SG. Non-apoptotic functions of BCL-2 family proteins. *Cell Death Differ*. 2017;24(8):1348–1358.
25. Hollville E, Carroll RG, Cullen SP, Martin SJ. Bcl-2 family proteins participate in mitochondrial quality control by regulating Parkin/PINK1-dependent mitophagy. *Mol Cell*. 2014;55(3):451–466. doi:10.1016/j.molcel.2014.06.001
26. Ji LL, Yeo D. Mitochondrial dysregulation and muscle disuse atrophy. *F1000Res*. 2019;8. doi:10.12688/f1000research.19139.1
27. Narendra DP, Youle RJ. Targeting mitochondrial dysfunction: role for PINK1 and Parkin in mitochondrial quality control. *Antioxid Redox Signal*. 2011;14(10):1929–1938. doi:10.1089/ars.2010.3799
28. Vargas JNS, Wang C, Bunker E, et al. Spatiotemporal control of ULK1 activation by NDP52 and TBK1 during selective autophagy. *Mol Cell*. 2019;74(2):347–362.e346. doi:10.1016/j.molcel.2019.02.010
29. Meyer N, Zielke S, Michaelis JB, et al. AT 101 induces early mitochondrial dysfunction and HMOX1 (heme oxygenase 1) to trigger mitophagic cell death in glioma cells. *Autophagy*. 2018;14(10):1693–1709. doi:10.1080/15548627.2018.1476812
30. Manni ME, Rigacci S, Borch E, et al. Monoamine oxidase is over-activated in left and right ventricles from ischemic hearts: an intriguing therapeutic target. *Oxid Med Cell Longev*. 2016;2016:4375418. doi:10.1155/2016/4375418

31. Ross JM. Visualization of mitochondrial respiratory function using cytochrome c oxidase/succinate dehydrogenase (COX/SDH) double-labeling histochemistry. *J Vis Exp*. 2011;57:e3266.
32. Wei R, Cao J, Yao S. Matrine promotes liver cancer cell apoptosis by inhibiting mitophagy and PINK1/Parkin pathways. *Cell Stress Chaperones*. 2018;23(6):1295–1309.
33. Martinez-Outschoorn UE, Pestell RG, Howell A, et al. Energy transfer in “parasitic” cancer metabolism: mitochondria are the powerhouse and Achilles’ heel of tumor cells. *Cell Cycle*. 2011;10(24):4208–4216. doi:10.4161/cc.10.24.18487
34. Ha S, Jeong SH, Yi K, et al. Phosphorylation of p62 by AMP-activated protein kinase mediates autophagic cell death in adult hippocampal neural stem cells. *J Biol Chem*. 2017;292(33):13795–13808. doi:10.1074/jbc.M117.780874
35. Park H, Chung KM, An HK, et al. Parkin promotes mitophagic cell death in adult hippocampal neural stem cells following insulin withdrawal. *Front Mol Neurosci*. 2019;12:46. doi:10.3389/fnmol.2019.00046
36. Wang T, Zhu Q, Cao B, Yuan Y, Wen S, Liu Z. Cadmium induces mitophagy via AMP-activated protein kinases activation in a PINK1/Parkin-dependent manner in PC12 cells. *Cell Prolif*. 2020;53(6):e12817. doi:10.1111/cpr.12817
37. Li Q, Gao S, Kang Z, et al. Rapamycin enhances mitophagy and attenuates apoptosis after spinal ischemia-reperfusion injury. *Front Neurosci*. 2018;12:865. doi:10.3389/fnins.2018.00865
38. Chourasia AH, Macleod KF. Tumor suppressor functions of BNIP3 and mitophagy. *Autophagy*. 2015;11(10):1937–1938. doi:10.1080/15548627.2015.1085136
39. Chen ZH, Lam HC, Jin Y, et al. Autophagy protein microtubule-associated protein 1 light chain-3B (LC3B) activates extrinsic apoptosis during cigarette smoke-induced emphysema. *Proc Natl Acad Sci U S A*. 2010;107(44):18880–18885. doi:10.1073/pnas.1005574107
40. Rizzieri D, Paul B, Kang Y. Metabolic alterations and the potential for targeting metabolic pathways in the treatment of multiple myeloma. *J Cancer Metastasis Treat*. 2019;5.
41. Dong K, Lei Q, Guo R, et al. Regulating intracellular ROS signal by a dual pH/reducing-responsive nanogels system promotes tumor cell apoptosis. *Int J Nanomedicine*. 2019;14:5713–5728. doi:10.2147/IJN.S208089

## Drug Design, Development and Therapy

Dovepress

### Publish your work in this journal

Drug Design, Development and Therapy is an international, peer-reviewed open-access journal that spans the spectrum of drug design and development through to clinical applications. Clinical outcomes, patient safety, and programs for the development and effective, safe, and sustained use of medicines are a feature of the journal, which has also

been accepted for indexing on PubMed Central. The manuscript management system is completely online and includes a very quick and fair peer-review system, which is all easy to use. Visit <http://www.dovepress.com/testimonials.php> to read real quotes from published authors.

Submit your manuscript here: <https://www.dovepress.com/drug-design-development-and-therapy-journal>